



Numerical Simulation of Heat Transfer Development of Nanofluids in a Thin Film over a Stretching Surface

Zaffer Elahi¹ · Muhammad Tahir Iqbal¹ · Azeem Shahzad¹ 

Received: 8 June 2021 / Accepted: 12 November 2021 / Published online: 19 January 2022
© The Author(s) under exclusive licence to Sociedade Brasileira de Física 2022

Abstract

This article focused on heat transfer analysis of nanofluid in a thin liquid film over an unsteady stretching surface. By means of the similarity transformations, the governing partial differential equations are converted into a set of ordinary differential equations. Solution of the resulting system is obtained by using Bvp4c in MATLAB. The impact of physical parameters, such as Prandtl, Eckert, and biot numbers on temperature profile, is explored graphically and interpreted physically for various nanofluids. This study revealed that nanofluid possesses maximum (minimum) thermal conductivity for $SiO_2(Ag)$ nanofluids, respectively. Further, the numerical simulation of skin friction coefficient and Nusselt number is carried out in tabular form and discussed in detail.

Keywords Thin film · Nanofluid · Heat transfer · Convective boundary conditions

Nomenclature

u, v	Velocity components along x, y directions
$h(t)$	Film thickness
α, b	Dimensional constants
U_w	Surface velocity
T_s	Surface temperature
T_r	Reference temperature
T_0	Slit temperature
κ_f	Thermal conductivity of the base fluid
κ_{nf}	Thermal conductivity of the nanofluid
C_p	Specific heat of fluid
Nu	Nusselt number
Re	Reynolds number
Pr	Prandtl number
B_0	Magnetic field
η	Similarity variable
ϕ	Volume fraction of nanoparticles
α_f	Thermal diffusion of water
α_{nf}	Thermal diffusion of nanofluid
ρ_f	Density of base fluid (water)
ρ_{nf}	Density of nanofluid

μ_f	Dynamic viscosity of water
μ_{nf}	Dynamic viscosity of nanofluid
ν_f	Kinematic viscosity of water
ν_{nf}	Kinematic viscosity of nanofluid
σ_{nf}	Electrical conductivity
$(\rho C_p)_{nf}$	Heat capacity of nanofluid

1 Introduction

Nanoscience and nanotechnology have played a vital role in energizing the conventional energy industries and stimulating the emerging renewable energy industries. All the forms of energy we are using today, out of which more than 70% are produced in or through the form of heat. In industry, heat must be passed either to inject energy into a system or to remove the produced energy from a system. That is why, the heat transfer process has become an important part in the era of nano-science and-technology. Nanotechnology was presented by Nobel laureate Feynman [1] during his well-known lecture “Plenty of Room at the Bottom.” Choi [2] gave the concept of “nanofluids” that are thinned suspensions of nanoparticles less than 100nm belonging to the new class of composite materials developed about last two decades ago by aiming the increase in thermal conductivity of heat transfer fluids.

The credit of enhancement in thermal conductivity completely goes to nanofluids which was initially reported since

✉ Azeem Shahzad
azeem.shahzad@uettaxila.edu.pk

Zaffer Elahi
zaffer.elahi@uettaxila.edu.pk

¹ Department of Basic Sciences, University of Engineering and Technology, Taxila 47050, Pakistan

last decade, in spite of much controversial debates and discrepancies, though the deficiency to formulate the mechanism of nanofluids wedged their application [3]. The rapid progress on nanofluids tells us how these deficiencies have been cleared. Nanofluids can be encountered in nuclear reactors, automobile, cooling of electronic devices, micro and mini channels, and renewable energy systems to enhance the performance characteristics of engineering devices [4–7]. Later on, homogeneous models [8, 9], the dispersion model [10] and the Buongiorno model [11] have been proposed to enhance the thermal conductivity of fluids(or nanofluids) using with (or without) nanoparticles, respectively. The flow and heat transfer in a thin liquid film over a stretching surface has also many applications in thermal engineering, such as fiber glass production, polymeric sheets, lubricants performance, roofing shingles, paper production, insulating materials, and condensation process [11–16]. Khan et al. [17] investigated the effects of variable viscosity and thermal conductivity on the flow and heat transfer in a laminar liquid film over horizontal stretching sheet. Noghrehabadi et al. [18] studied the slip effects on the boundary layer flow and heat transfer over a stretching surface based on nanoparticle fractions. Moreover, the numerical and analytical studies upon nanofluids with slip conditions have been found in [19–24].

It should be noted that the convective heat transfer characteristic of nanofluids depends on the thermophysical properties of the flow pattern and flow structure of the base fluid, the volume fraction of suspended particles, the dimensions and the shape of nanoparticles. The thermophysical properties, shape factor, and viscosity coefficients of different nanoparticles with water as base fluid are given in Tables 1 and 2.

The thermal conductivity and viscosity models of metallic oxides nanofluids were presented by Alawi et al. [25]. Maiga et al. [26] observed heat transfer enhancement using nanofluids inforced convection flow. Tiwari and Das [27] proposed heat transfer augmentation in a two-sided lid-driven differentially heated square cavity utilizing nanofluids. Dinarvand

Table 1 Thermophysical properties of base fluid and nanoparticles [31]

Nanoparticles	Density (kg/m^3)	Thermal conductivity ($W/m K$)	Specific heat ($J/kg K$)	Electrical conductivity (S/m)
Cu	8933	401	385	59.6
Ag	10500	429	235	63.0
H_2O	997.1	0.613	4179	5.50
SiO_2	2200	1.2	703	0.0000055
TiO_2	4250	8.9538	686.2	0.125
Al_2O_3	3970	40	765	16.5

Table 2 Viscosity and shape factor value of nanoparticle [32]

Nanoparticle	Viscosity A_1	Coefficients A_2	Shape factor m
Spherical	2.5	6.5	3.0

et al. [28] Buongiorno’s model for double-diffusive mixed convective stagnation-point flow of a nanofluid considering diffusio-phoresis effect of binary base fluid. Tzou [29] reported thermal instability of nanofluids in natural convection. Oztop and Abu-Nada [30] discussed numerical study of natural convection in partially heated rectangular enclosures filled with nanofluids.

It has been seen clearly, from the cited literature, that the majority of the researchers analyze the thermal conductivity of different nanofluids over a stretching surface under various physical constraints. To the best of our knowledge, no study has been carried out for the development of thermal conductivity in thin film over a stretching surface along with convective conditions for different nanofluids.

The rest of article is organized as follows; the detailed description of the proposed model is discussed in Sect. 2. Dimensionless form of the model with physical quantities including similarity transformations are interpreted in Sect. 3 and its subsections, while the method of solution of the model with numerical technique Bvp4c is explained in Sect. 4. The pertinent features of the physical quantities are presented in Sect. 5 and its subsections. Finally, the concluding remarks are summarized in Sect. 6.

2 Mathematical Modeling of the Problem

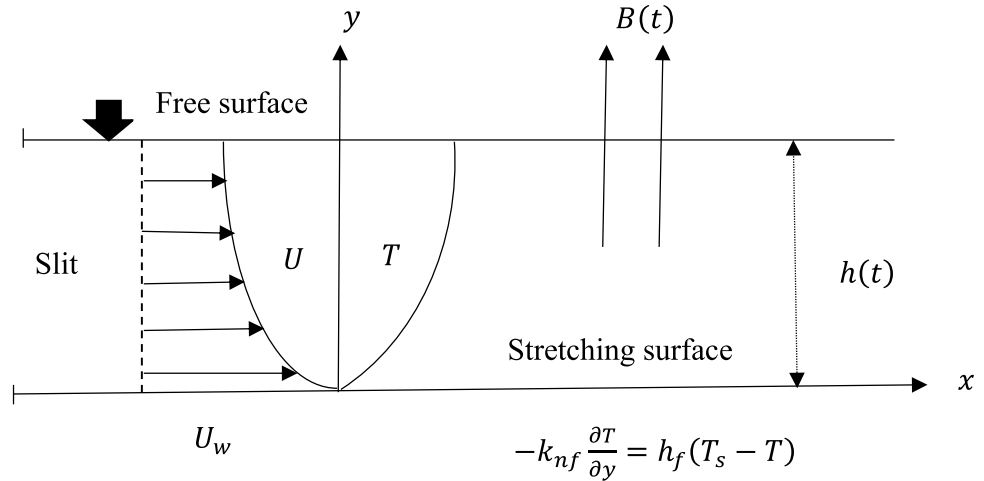
Consider a two-dimensional time dependent fluid flow and heat transfer in a thin film over a stretched surface attached with a slit. The rectangular coordinate system is chosen in such a way that x -axis and y -axis is taken along and normal to the surface, respectively. The assumed base nanofluid (water) with spherical shape nanoparticles, $Cu, Ag, Al_2O_3, SiO_2, TiO_2$ is considered in thermal equilibrium, and moves with uniform velocity $U_w = \frac{bx}{1-\alpha t}$ in x -direction due to stretching of surface. Film thickness is taken as $h(t)$, while the temperature distribution at the wall is given by

$$T_s = T_0 - T_r \left(\frac{bx^2}{2\nu_f} \right) (1 - \alpha t)^{\frac{-3}{2}},$$

where

- α, b = Dimensional constants,
- T_r = Reference temperature,
- T_0 = Slit temperature,
- ν_f = Kinematic viscosity of base fluid.

Fig. 1 Diagram of physical model with boundary conditions



The uniform magnetic field $B(t) = \frac{B_0}{\sqrt{1-\alpha t}}$ is applied perpendicularly to the surface, as shown in Fig. 1.

Assume coordinates axes are labeled with the respective velocity components, as $u = u(x, y, t)$, $v = v(x, y, t)$, and temperature of the nanofluid is $T = T(x, y, t)$. With all these suppositions, the equations of continuity, momentum, and energy are grabbed by following the Tiwari and Das model [27];

$$\frac{\partial u}{\partial x} + \frac{\partial v}{\partial y} = 0, \tag{1}$$

$$\frac{\partial u}{\partial t} + u \frac{\partial u}{\partial x} + v \frac{\partial u}{\partial y} = \frac{\mu_{nf}}{\rho_{nf}} \frac{\partial^2 u}{\partial y^2} - \frac{\sigma_{nf}}{\rho_{nf}} B(t)^2 u, \tag{2}$$

$$\frac{\partial T}{\partial t} + u \frac{\partial T}{\partial x} + v \frac{\partial T}{\partial y} = \alpha_{nf} \frac{\partial^2 T}{\partial y^2} + \frac{\mu_{nf}}{\rho_{nf} C_p} \left(\frac{\partial u}{\partial y} \right)^2, \tag{3}$$

subject to the boundary conditions

$$u = U_w + Av_f \frac{\partial u}{\partial y}, \quad v = 0, \quad -\kappa_{nf} \frac{\partial T}{\partial y} = h_f (T_0 - T) \text{ at } y = 0, \tag{4}$$

$$\frac{\partial u}{\partial y} = 0, \quad \frac{\partial T}{\partial y} = 0, \quad v = \frac{dh}{dt} \text{ at } y = h(t), \tag{5}$$

where

A = Proportionality constant, h_f = Convective heat coefficient.

The thermophysical properties of the hybrid nanofluid defined in [33, 34] can be written as

$$\left. \begin{aligned} \alpha_{nf} &= \frac{\kappa_{nf}}{(\rho C_p)_{nf}}, & \rho_{nf} &= (1 - \phi)\rho_f + \phi\rho_s, & \mu_{nf} &= \mu_f(1 + A_1\phi + A_2\phi^2), \\ \sigma_{nf} &= \sigma_f(1 - \phi)\sigma_f + \phi\sigma_s, & (\rho C_p)_{nf} &= (1 - \phi)(\rho C_p)_f + \phi(\rho C_p)_s, \end{aligned} \right\} \tag{6}$$

and

$$\frac{\kappa_{nf}}{\kappa_f} = \left[\frac{\kappa_s + (m - 1)\kappa_f + (m - 1)(\kappa_s - \kappa_f)\phi}{\kappa_s + (m - 1)\kappa_f - (\kappa_s - \kappa_f)\phi} \right], \tag{7}$$

where

$(\rho C_p)_{nf}$ = Heat capacity,

ϕ = Volume fraction of nanofluid,

A_1, A_2 = Viscosity coefficients of enhancing heat capacitance.

Moreover, κ_s and m are the thermal conductivity and shape factor of the nanoparticle, and thermophysical properties of base fluid, nanofluid, and nanoparticles of solids are represented by f, nf and s .

3 Dimensionless Model

The non-dimensional form of the complete model with physical quantities have been presented in the following subsections.

3.1 Similarity Transformations

Introducing the transformations

$$\left. \begin{aligned} T &= T_0 - T_r \left(\frac{bx^2}{2v_f} \right) (1 - \alpha t)^{-\frac{3}{2}} \theta(\eta), \\ \eta &= \left(\frac{b}{v_f(1 - \alpha t)} \right)^{\frac{1}{2}} y, \\ \psi &= \left(\frac{bv_f}{1 - \alpha t} \right)^{\frac{1}{2}} x f(\eta), \end{aligned} \right\} \tag{8}$$

where the flow pattern is described by a stream function ψ , defined as

$$u = \frac{\partial \psi}{\partial y}, \quad v = -\frac{\partial \psi}{\partial x},$$

that trivially satisfy the continuity Eq. (1). The following coupled nonlinear system has been found by means of transformations (8) into (2–5), as

$$\epsilon_1 f'''(\eta) - M \epsilon_3 f'(\eta) + \left[f(\eta) f''(\eta) - f'^2(\eta) - S \left(f'(\eta) + \frac{\eta}{2} f''(\eta) \right) \right] = 0, \tag{9}$$

$$\frac{\epsilon_2}{Pr} \theta''(\eta) + Ec \epsilon_3 f'^2(\eta) + \left[f(\eta) \theta'(\eta) - 2\theta(\eta) f'(\eta) - \frac{S}{2} (3\theta(\eta) + \eta \theta'(\eta)) \right] = 0, \tag{10}$$

subject to convective boundary conditions

$$\left. \begin{aligned} f(0) = 0, \quad f'(0) = 1 + K f''(0), \quad \theta'(0) = -\gamma \frac{\kappa_f}{\kappa_{nf}} (1 - \theta(0)), \quad \text{at } \eta = 0, \\ f(\beta) = \frac{S\beta}{2}, \quad f''(\beta) = 0, \quad \theta'(\beta) = 0, \quad \text{at } \eta = \beta. \end{aligned} \right\} \tag{11}$$

3.2 Physical Quantities

The dimensionless form of physical quantities, such as slip, magnetic, and unsteadiness parameters, and Eckert, Prandtl, and biot numbers, respectively, have been given here under:

$$\begin{aligned} K &= A \sqrt{\frac{v_f U_w}{x}}, \quad M = \frac{\beta_0^2 \sigma_f}{b \rho_{nf}}, \quad S = \frac{\alpha}{b}, \\ \gamma &= \frac{h_f}{\kappa_f} \left(\frac{x v_f}{U_w} \right)^{\frac{1}{2}}, \quad Ec = \frac{U_w^2}{C_p (T_s - T)}, \\ Pr &= \frac{(\rho C_p)_f v_f}{\kappa_f}. \end{aligned}$$

The constants ϵ_i , $i = 1, \dots, 3$ containing the solid volume fraction ϕ , defined as

$$\epsilon_1 = \frac{1 + A_1 \phi + A_2 \phi^2}{1 - \phi + \phi \left(\frac{\rho_s}{\rho_f} \right)}, \quad \epsilon_2 = \frac{\left(\frac{\kappa_{nf}}{\kappa_f} \right)}{1 - \phi + \phi \left(\frac{\rho C_{p_s}}{\rho C_{p_f}} \right)}, \quad \epsilon_3 = \frac{1 - \phi + \phi \left(\frac{\sigma_s}{\sigma_f} \right)}{1 - \phi + \phi \left(\frac{\rho_s}{\rho_f} \right)}. \tag{12}$$

In addition, the skin friction and Nusselt number can be written, instructively, as

$$C_f = \frac{\tau_w}{\rho_f U_w^2}, \quad Nu = \frac{x q_w}{\kappa_f (T_s - T_0)}, \tag{13}$$

with

$$\tau_w = \mu_{nf} \left[\frac{\partial u}{\partial y} \right]_{y=0}, \quad q_w = -\kappa_{nf} \left[\frac{\partial T}{\partial y} \right]_{y=0}.$$

The dimensionless form of (13) by means of transform variables is given by:

$$Re^{\frac{1}{2}} C_f = (1 + A_1 \phi + A_2 \phi^2) f''(0), \quad Re^{-\frac{1}{2}} Nu = -\frac{\kappa_{nf}}{\kappa_f} \theta'(0). \tag{14}$$

4 Solution Methodology

In order to solve the coupled nonlinear system (9–11) numerically, the set of first-order linear equations has been found by considering

$$f = g_0, \tag{15}$$

$$g'_0 = g_1, \tag{16}$$

$$g'_1 = g_2, \tag{17}$$

$$g'_2 = \epsilon_1^{-1} \left[S \left(g_1 + \frac{\eta}{2} g_2 \right) + g_1^2 - g_0 g_2 + M \epsilon_3 g_1 \right], \tag{18}$$

$$\theta = g_3, \tag{19}$$

$$g'_3 = g_4, \tag{20}$$

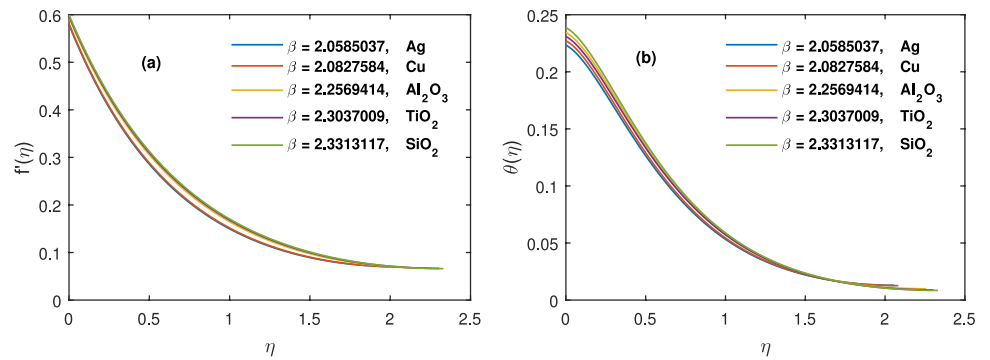
$$g'_4 = Pr \epsilon_2^{-1} \left[\frac{S}{2} (3g_3 + \eta g_4) + 2g_1 g_3 - g_0 g_4 - Ec \epsilon_1 g_2^2 \right], \tag{21}$$

$$g_0(0) = 0, \quad g_0(\beta) = \frac{S\beta}{2}, \quad g_1(0) = 1 + K g_2(0), \quad g_2(\beta) = 0, \tag{22}$$

$$g_4(\beta) = 0, \quad g_4(0) = -\gamma \frac{\kappa_f}{\kappa_{nf}} (1 - g_3(0)), \tag{23}$$

leads to a system of first-order equations subject to six boundary conditions. Initially, solve the Eqs. (16–18) and (22) with suitable guess of β which is given by the program Bvp4c in MATLAB, yields a relationship between S and β that reduces the number of boundary conditions. The β value is then chosen in such a way that satisfy the condition $g_0(\beta) = \frac{S\beta}{2}$ which is done by hit and trail method. Finally, the above system of Eqs. (16–21) along with conditions (22) and (23) is then solved for known values of S and β using Bvp4c in MATLAB. More detail on Bvp4c with convergence and error analysis have been found in [35–39], and the references there in.

Fig. 2 Comparisons of velocity and temperature profiles of different nanoparticles

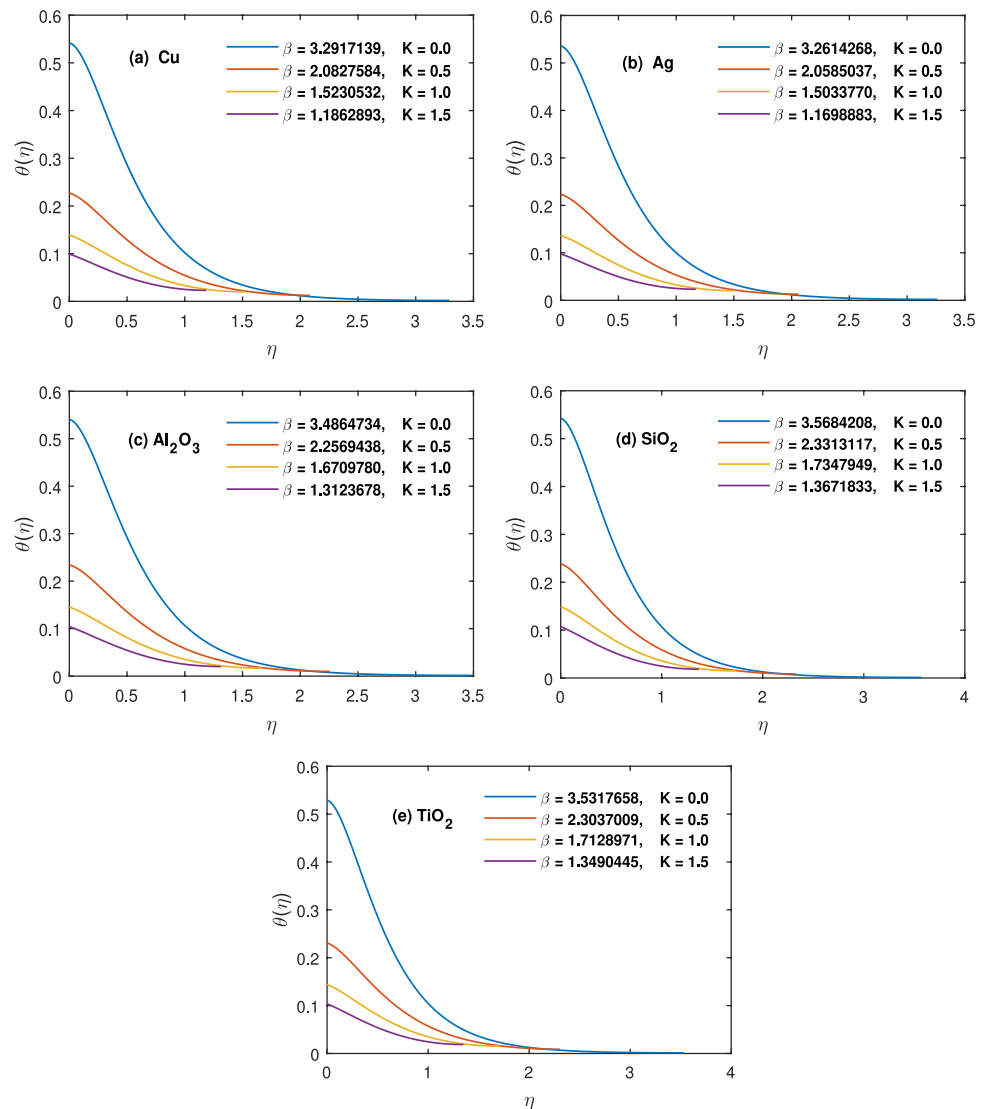


5 Results and Discussion

This section presents the analysis of thermal conductivity and effect of significant quantities in thin film of nano-fluid by stretching a surface. The following subsections

depicted results of velocity $f'(\eta)$ and temperature $\theta(\eta)$ profiles, and interpreted using slip parameter K , unsteadiness parameter S , volume fraction ϕ , biot number γ , Eckert number Ec , Prandtl number Pr .

Fig. 3 Temperature profiles for different values of slip parameter at $S = 0.4, M = 1.0, \phi = 0.02, \gamma = 0.1, Pr = 6.0, Ec = 1.0$



5.1 Graphical Simulation

Comparison of velocity and temperature profiles of each nanosize particle are shown in Fig. 2(a) and (b) that inferred the velocity and temperature fields with film thickness β are getting rise by changing the nanoparticles continuously. It should also be noticed that both velocity and temperature fields with film thickness β are high for SiO_2 nanoparticles of spherical-shape.

Figure 3(a–e) shows the comparison among different nanosize particles on temperature profile using different values of slip parameter K . It is shown in the graph that the rise in slip parameter K causes the curve to shift toward low-temperature profile for all nanoparticles and the thickness of boundary layer decreases as a consequence.

Figure 4(a–e) represents the case of unsteadiness parameter S on temperature profile $\theta(\eta)$ in the boundary layer. It

can be observed that increase in unsteadiness parameter S declines the temperature profile. This implies that the enhancement in unsteadiness parameter reduces thermal boundary layer thickness which is due to variation in fluid viscosity decreasing the effect of buoyant forces of gravity. As a result, shear thinning is observed. In other words, the rise in unsteadiness parameter causes the reduction of heat transfer from the stretching sheet to the film in the boundary layer region.

The effect of volume fraction ϕ on temperature profile is analyzed in Fig. 5(a–e) for different nanoparticles. It is evident from the graph that the temperature profile is the decreasing function of volume fraction regardless of the type of nanoparticles. This behavior points to decrease in thermal conductivity due to increase in ϕ . It should be mentioned here that the thermal conductivity is highly enhanced in the cases of SiO_2, Al_2O_3, TiO_2 as compared to Cu and Ag . This indicates the effect of augmented heat transfer and specific

Fig. 4 Temperature profiles for different values of unsteadiness parameter at $K = 0.5, M = 1.0, \phi = 0.02, \gamma = 0.1, Pr = 6.0, Ec = 1.0$

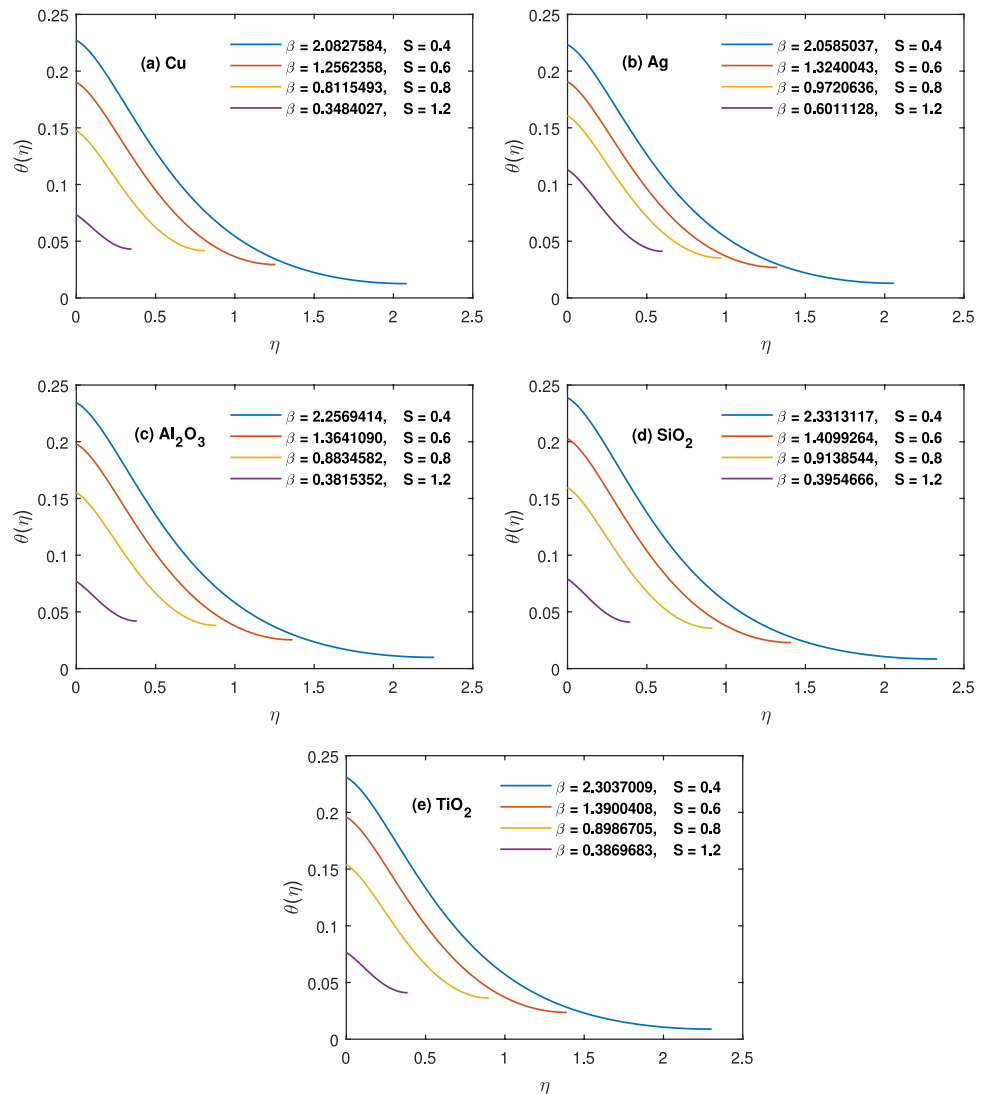
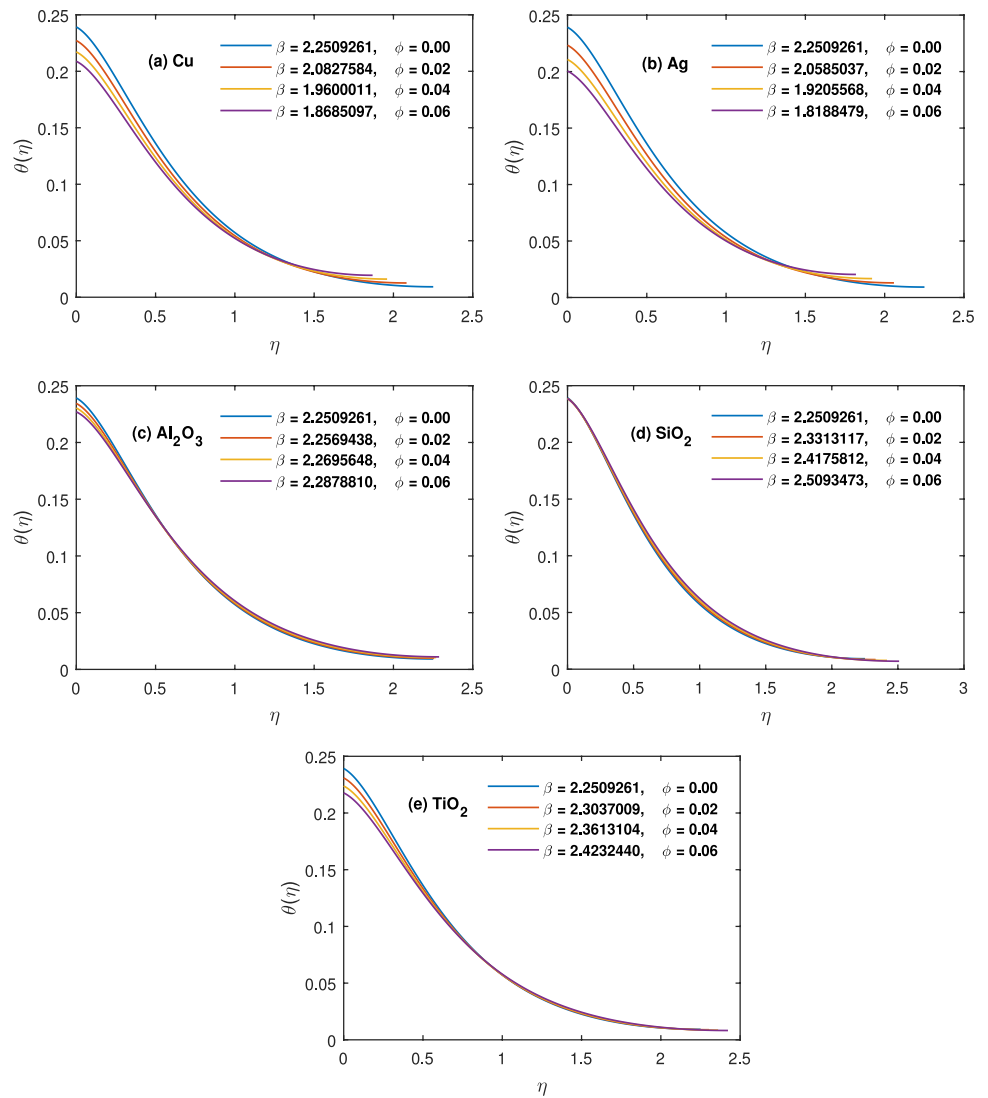


Fig. 5 Temperature profiles for different values of volume fraction at $K = 0.5, S = 0.4, M = 1.0, \gamma = 0.1, Pr = 6.0, Ec = 1.0$



heat. Also, SiO_2 nanoparticles exhibit great efficiency in controlling the temperature variations for different practical situations.

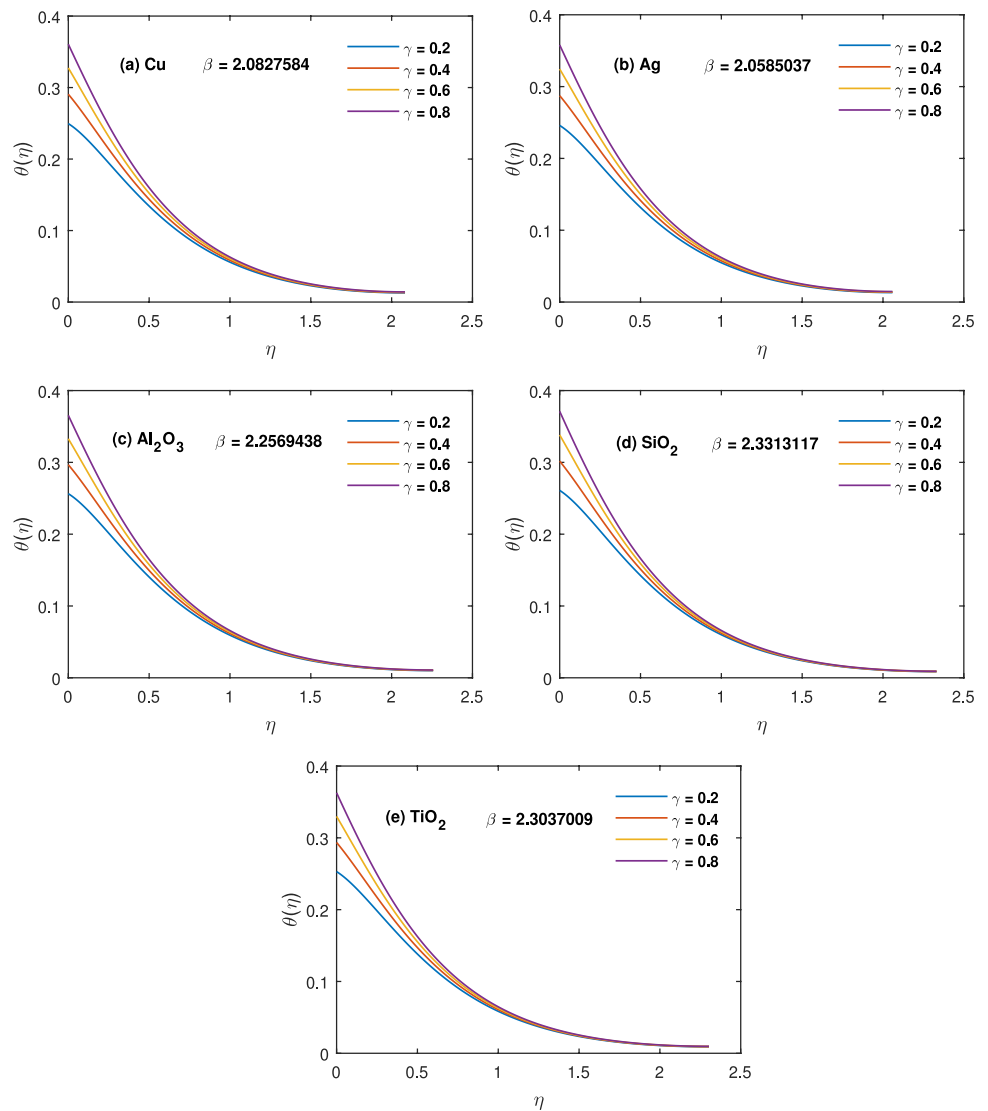
Figure 6(a–e) elucidates the influence of biot number γ on temperature profile. A stronger convection at high temperature and thermal boundary layer thickness is a result of increase in γ . Physically, the relationship between the convection at the surface to the conduction within the surface is named as biot number. When the thermal gradient is applied to the stretching surface, then the ratio governing the temperature inside a surface varies significantly, while the surface heats or cools over time.

Figure 7(a–e) shows the increasing trend of Eckert number Ec on decreasing temperature profile $\theta(\eta)$. Increase in Ec number enhances the heat dissipation potential but diminishes the temperature gradient between the sheet and the fluid film by the cause of

frictional heating. Hence, heat transfer rate decreases with the increment of Ec number. Physically, much random motion of different nanosize particles are linked with higher values of Ec that results in enhancement of temperature. However, $Ec = 1$ points to reversion in the direction of heat transfer and change in temperature gradient sign.

Figure 8(a–e) shows that by varying Prandtl number Pr , the temperature profile is successively getting increased from Cu to SiO_2 . It is worth mentioning that the temperature value is high for SiO_2 nanosize particle. Physically, larger Prandtl fluids possess weaker thermal diffusivity as surrounding temperature becomes equal to the surface temperature and vice versa. So, a reduction in the temperature and thermal boundary layer thickness is due to the change in thermal diffusivity and it prevents spreading of heat in the fluid declining the heat transfer rate.

Fig. 6 Temperature profiles for different values of biot number at $K = 0.5, S = 0.4, M = 1.0, \phi = 0.02, Pr = 6.0, Ec = 1.0$



5.2 Numerical Simulation

This section includes the numerical simulations of skin friction coefficient and Nusselt number along with comparison of present results with the existing ones from the literature.

Table 3 reveals the decreasing values of skin friction coefficient for different spherical-shaped nanosize particles against the rising value in slip parameter K and unsteadiness parameter S , while a reverse trend is seen for volume fraction parameter ϕ and magnetic parameter M .

In addition, the rate of heat transfer at the surface is given in Table 4. It is inferred that the Nusselt number is decreased for each spherical-shaped nanoparticle corresponding to Prandtl and Eckert numbers, as well. Particularly, the Nusselt number is grown up for both unsteadiness and biot number.

Finally, the present results have been compared with Andersson et al. [40], Chen [41–43], Wang and Pop [44] and Li et al. [45] and are cited in Table 5.

Fig. 7 Temperature profiles for different values of Eckert number at $K = 0.5, S = 0.4, M = 1.0, \phi = 0.02, \gamma = 0.1, Pr = 6.0$

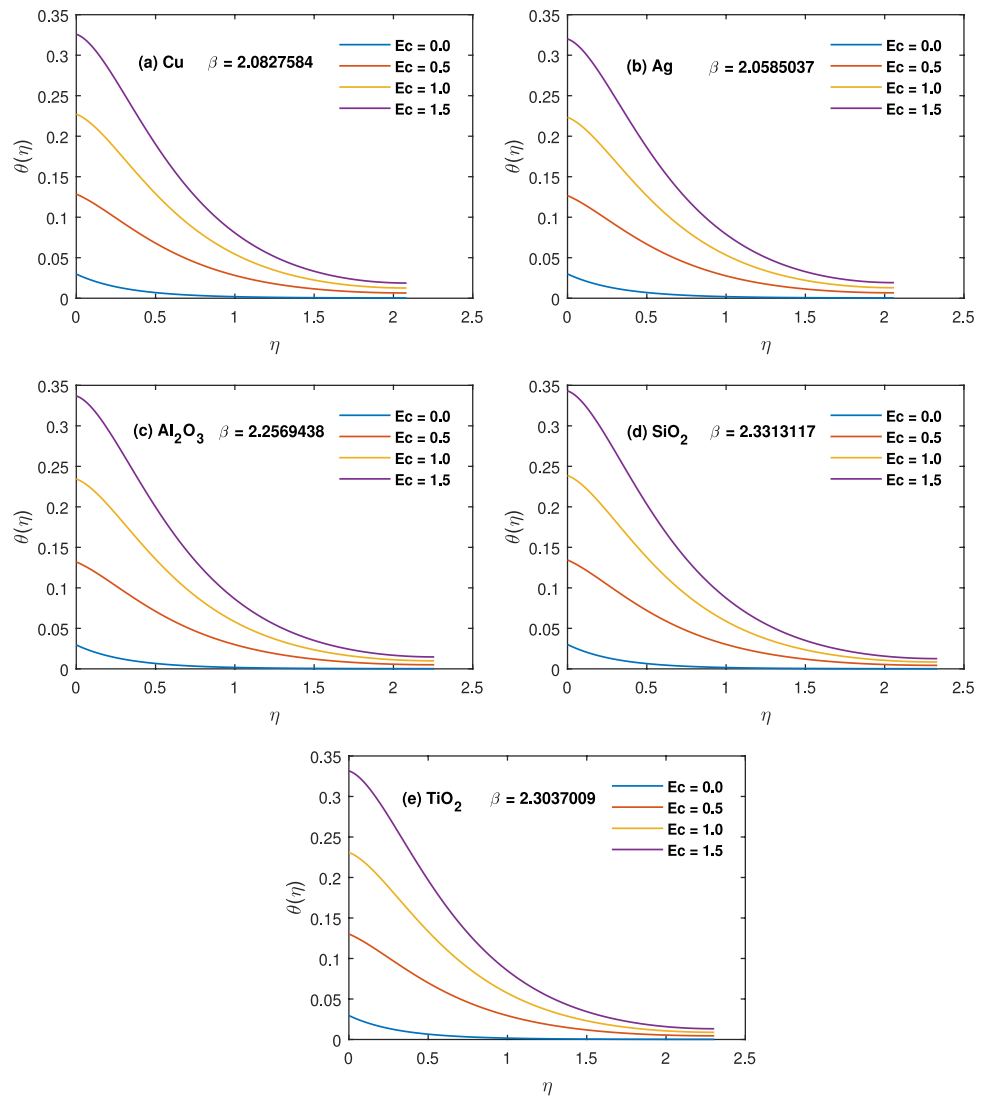


Fig. 8 Temperature profiles for different values of Prandtl at $K = 0.5, S = 0.4, M = 1.0, \phi = 0.02, \gamma = 0.1, Ec = 1.0$

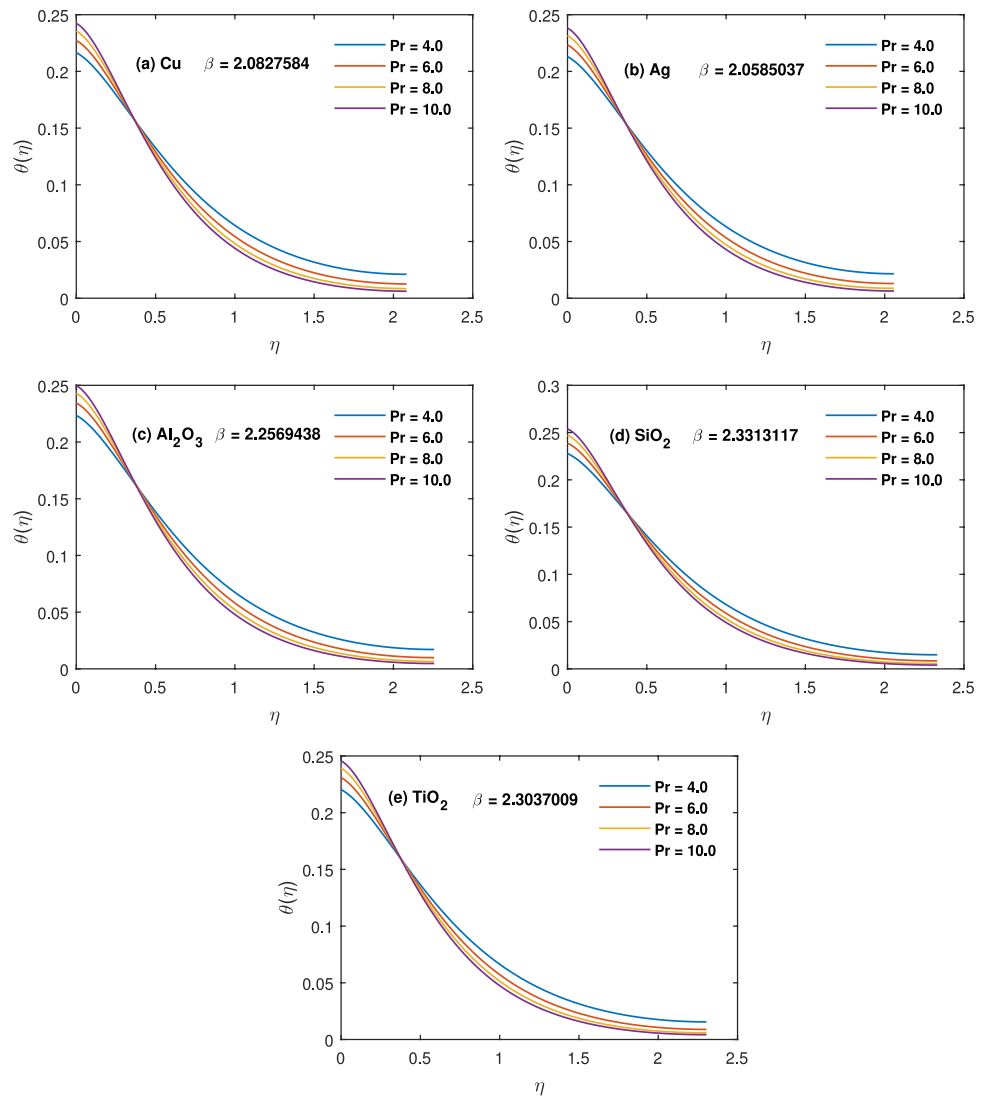


Table 3 Numerical results of skin friction coefficient of different nanoparticles

Physical quantities				Cu	Ag	Al_2O_3	SiO_2	TiO_2
K	ϕ	M	S	$-Re^{\frac{1}{2}} C_f$				
0.0	0.02	1.0	0.4	1.6844796	1.7009423	1.5927428	1.5573284	1.5753015
0.5	-	-	-	0.8817619	0.8860123	0.8541049	0.8429735	0.8475353
1.0	-	-	-	0.6047180	0.6066373	0.5912814	0.5857601	0.5877835
0.5	0.00	1.0	0.4	0.8121426	0.8121426	0.8121426	0.8121426	0.8121426
-	0.02	-	-	0.8817619	0.8860123	0.8541405	0.8429735	0.8475353
-	0.04	-	-	0.9523268	0.9600767	0.8991151	0.8762580	0.8857592
0.5	0.02	0.0	0.4	0.7116873	0.7173195	0.6929123	0.6858401	0.6940121
-	-	0.5	-	0.8088970	0.8155188	0.7844299	0.7747844	0.7806811
-	-	1.0	-	0.8817619	0.8860123	0.8541049	0.8429735	0.8475353
0.5	0.02	1.0	0.6	0.8818025	0.8906614	0.8561205	0.8457757	0.8505131
-	-	-	0.8	0.8529044	0.8851230	0.8309913	0.8221338	0.8266602
-	-	-	1.2	0.6871882	0.8499777	0.6756896	0.6709830	0.6738603

Table 4 Numerical results of Nusselt number of different nanoparticles

Physical quantities						Cu	Ag	Al_2O_3	SiO_2	TiO_2
K	ϕ	Ec	S	Pr	γ			$Re^{-\frac{1}{2}}Nu$		
0.0	0.02	1.0	0.4	6.0	0.1	0.04581959	0.04643369	0.04592300	0.04572684	0.04707365
0.5	-	-	-	-	-	0.07728078	0.07766514	0.07655661	0.07612269	0.07690809
1.0	-	-	-	-	-	0.08608445	0.08632313	0.08546456	0.08509051	0.08560481
0.5	0.00	1.0	0.4	6.0	0.1	0.07607385	0.07607385	0.07607385	0.07607385	0.07607385
-	0.02	-	-	-	-	0.07728078	0.07766514	0.07655661	0.07612269	0.07690809
-	0.04	-	-	-	-	0.07828170	0.07893059	0.07696088	0.07614112	0.07761780
0.5	0.02	0.0	0.4	6.0	0.1	0.09701849	0.09700548	0.09704885	0.09699551	0.09704589
-	-	0.5	-	-	-	0.08714963	0.08733529	0.08680273	0.08655909	0.08697699
-	-	1.0	-	-	-	0.07728078	0.07766514	0.07655661	0.07612269	0.07690809
0.5	0.02	1.0	0.6	6.0	0.1	0.08098130	0.08094375	0.08018569	0.07972574	0.08041330
-	-	-	0.8	-	-	0.08526068	0.08392977	0.08448550	0.08404190	0.08460445
-	-	-	1.2	-	-	0.09266706	0.08869798	0.09231836	0.09209853	0.09234914
0.5	0.02	1.0	0.4	4.0	0.1	0.07834525	0.07869844	0.07765579	0.07721767	0.07796518
-	-	-	-	6.0	-	0.07728078	0.07766514	0.07655661	0.07612269	0.07690809
-	-	-	-	8.0	-	0.07644263	0.07684640	0.07570610	0.07528070	0.07608996
0.5	0.02	1.0	0.4	6.0	0.2	0.13647948	0.13822615	0.14263917	0.14456770	0.14940266
-	-	-	-	-	0.4	0.25857074	0.26179928	0.26991035	0.27342353	0.28258844
-	-	-	-	-	0.6	0.36843515	0.37293211	0.38417023	0.38899687	0.40206181

Table 5 Comparison of present results when $M = K = \phi = 0$

S	Andersson et al. [40]		Chen [41–43]		Wang and Pop [44]		Lin et al. [45]		Present results	
	β	$-f''(0)$	β	$-f''(0)$	β	$-f''(0)$	β	$-f''(0)$	β	$-f''(0)$
0.8	2.15199	1.24581	2.1520	1.24581	2.15199	1.24580	2.1522	1.2457	2.152021	1.2458064
1.0					1.54362	1.27777	1.5438	1.2777	1.543615	1.2777693
1.2	1.12778	1.27917	1.1278	1.27918	1.12778	1.27918	1.1280	1.2790	1.127779	1.2791718

6 Conclusion

The heat transfer development of nanofluids in a thin film over a stretching surface subject to convective boundary condition has been manipulated using $Cu, Ag, Al_2O_3, TiO_2, SiO_2$ as nanoparticles of spherical-shape. The obtained results and their effects on both velocity and temperature fields have been elucidated through graphical simulations and tables. Moreover, the results have been verified by making a comparison with the existing ones that reveal the validity of the scheme. Thus, the main findings of the present work have been summarized, as under

- The velocity and temperature fields of spherical shaped SiO_2 nanoparticles are very high when compared to other types of nanoparticles with respect to the film thickness β while silver Ag nanoparticles was reported to have small velocity and temperature profiles.
- Physical quantities, such as slip parameter K , unsteadiness parameter S , Eckert number Ec and volume fraction ϕ showed decline in temperature profile for all nanoparticles when film thickness β was reduced. The SiO_2 nanoparticles were found to have highest heat transfer rate when compared to other nanoparticles.
- Decrease in heat transfer was observed for increasing volume fraction of nanoparticles, i.e., thermal conductivity was decreased with enhancement of particle concentration.
- Rise in biot number γ augmented the temperature profile against for each increasing value of film thickness β and lead to strong convection.
- The skin friction coefficient declines with slip boundary conditions and unsteadiness parameters, while augument for volume fraction parameter.
- The Nusselt number increases for slip parameter, unsteadiness parameter, and biot number but decreases for Prandtl and Eckert number.

Declarations

Conflicts of interest All the authors declare that they have no conflict of interest.

References

- R.P. Feynman, There's Penelty of room at the bottom. *Eng. Sci.* **23**(5), 22–36 (1960)
- S.U.S. Choi, Enhancing Thermal Conductivity of Fluids with Nanoparticles, in *Proceedings of the 1995 ASME International Mechanical Engineering Congress and Exposition San Francisco CA, USA* (1995)
- Wen et al., Review of nanofluids for heat transfer applications. *Particuology* **7**(2), 141–150 (2009)
- R. Saidur, K.Y. Leong, H.A. Mohammad, A review on applications and challenges of nanofluids. *Renew. Sust. Energ. Rev.* **15**(3), 1646–1668 (2011)
- Hung et al., Heat transfer enhancement in microchannel heat sinks using nanofluids. *Int. J. Heat Mass Transf.* **55**(9–10), 2559–2570 (2012)
- C.-J. Ho, W.-C. Chen, W.-M. Yan, Correlations of heat transfer effectiveness in a minichannel heat sink with water-based suspensions of Al_2O_3 nanoparticles and/or MEPCM particles. *Int. J. Heat Mass Transf.* **69**, 293–299 (2014)
- Esfe et al., ANN modeling, cost performance and sensitivity analyzing of thermal conductivity of DWCNT SiO_2 /EG hybrid nanofluid for higher heat transfer. *J. Therm. Anal. Calorim.* **131**(3), 2381–2393 (2017)
- J.A. Eastman, S.U.S. Choi, S. Li, W. Yu, L.J. Thompson, Anomalous increased effective thermal conductivities of ethylene glycol-based nanofluids containing copper nanoparticles. *Appl. Phys. Lett.* **78**, 718–720 (2001)
- S.E.B. Maïga, S.J. Palm, C.T. Nguyen, G. Roy, N. Galanis, Heat transfer enhancement by using nanofluids in forced convection flows. *Int. J. Heat Fluid Flow* **26**(4), 530–546 (2005)
- Y.M. Xuan, W. Roetzel, Conceptions for heat transfer correlation of nanofluids. *Int. J. Heat Transfer* **43**(19), 3701–3707 (2000)
- J. Buongiorno, Convective transport in nanofluids, *AMSE. J. Heat Transfer* **128**(3), 240–250 (2006)
- N. Sandeep, A. Malvandi, Enhanced heat transfer in liquid thin film flow of non-Newtonian nanofluids embedded with graphene nanoparticles. *Adv. Powder Technol.* **27**, 2448–2456 (2016)
- Fakour et al., Nanofluid thin film flow and heat transfer over an unsteady stretching elastic sheet by LSM. *J. Mech. Sci. Technol.* **32**(1), 177–183 (2018)
- Lin et al., MHD pseudo-plastic nanofluid unsteady flow and heat transfer in a finite thin film over stretching surface with internal heat generation. *Int. J. Heat and Mass Transf.* **84**, 903–911 (2015)
- G.K. Ramesh, G.S. Roopa, S. Shehzad, S.U. Khan, Interaction of $Al_2O_3 - Ag$ and $Al_2O_3 - Cu$ hybrid nanoparticles with water on convectively heated moving material. *Multidiscip. Model. Mater. Struct.* **16**(6), 1651–1667 (2020)
- G.K. Ramesh, Influence of shape factor on hybrid nanomaterial in a cross flow direction with viscous dissipation. *Phys. Scr.* **94**(10), 105–224 (2019)
- Y. Khan, Q.B. Wu, N. Faraz, A. Yildirim, The effects of variable viscosity and thermal conductivity on a thin film flow over a shrinking/ stretching sheet. *Comput. Math. Appl.* **60**, 3391–3399 (2011)
- A. Noghrehabadi, R. Pourrajab, M. Ghalambaz, Effect of partial slip boundary condition on the flow and heat transfer of nanofluids past stretching sheet prescribed constant wall temperature. *Int. J. Therm. Sci.* **54**, 253–261 (2012)
- A. Hussanan, M.Z. Salleh, I. Khan, Microstructure and inertial characteristics of a magnetite ferrofluid over a stretching/shrinking sheet using effective thermal conductivity model. *J. Mol. Liq.* **255**, 64–75 (2018)
- Kai-Long. Hsiao, Micropolar nanofluid flow with MHD and viscous dissipation effects towards a stretching sheet with multimedia feature. *Int. J. Heat Mass Transf.* **100**, 316–323 (2016)
- K. Hooman, A. Ejlali, Effects of viscous heating, fluid property variation, velocity slip, and temperature jump on convection through parallel plate and circular microchannels. *Int. Communi. in Heat Mass Transf.* **37**(1), 34–38 (2010)
- Hussanan et al., Slip effects on unsteady free convective heat and mass transfer flow with Newtonian heating. *Therm. Sci.* **26**(6), 1852–1939 (2016)
- A. Hamid, Hashim, M. Khan, Heat generation/absorption and velocity slip effects on unsteady axisymmetric flow of Williamson magneto-nanofluid. *Mod. Phys. Lett. B* **33**(34), 1950432 (2019)
- Iqbal et al., Magnetohydrodynamic thin film deposition of Carreau nanofluid over an unsteady stretching surface. *Appl. Phys. A* **126**(2) (2020). <https://doi.org/10.1007/s00339-019-3204-6>
- Alawi et al., Thermal conductivity and viscosity models of metallic oxides nanofluids. *Int. J. Heat Mass Transf.* **116**, 1314–1325 (2018)
- Maïga et al., Heat transfer enhancement by using nanofluids in forced convection flow. *Int. J. Heat. Fluid Flow* **26**(4), 530–546 (2005)
- R.J. Tiwari, M.K. Das, Heat transfer augmentation in a two-sided lid-driven differentially heated square cavity utilizing nanofluids. *Int. J. Heat Mass Transf.* **50**(9–10), 2002–2018 (2007)
- S. Dinarvand, R. Hosseini, M. Abulhasansari, I. Pop, Buongiorno's model for double-diffusive mixed convective stagnation-point flow of a nanofluid considering diffusio-phoresis effect of binary base fluid. *Adv. Powder Technol.* **26**, 1423–1434 (2015)
- D.Y. Tzou, Thermal instability of nanofluids in natural convection. *Int. J. Heat Mass Transf.* **51**, 2967–2979 (2008)
- H.F. Oztop, E. Abu-Nada, Numerical study of natural convection in partially heated rectangular enclosures filled with nanofluids. *Int. J. Heat Fluid Flow* **29**, 1326–1336 (2008)
- S.R. Vajjha, K.D. Debendra, Experimental determination of thermal conductivity of three nanofluids and development of new correlations. *Int. J. Heat Mass Transf.* **52**(21–22), 4675–4682 (2009)
- E.V. Timofeeva, J.L. Routbort, D. Singh, Particle shape effects on thermophysical properties of alumina nanofluids. *J. Appl. Physiol.* **106**(1), 014304 (2009)
- A. Hamid, M. Khan, Multiple solutions for MHD transient flow of Williamson nanofluids with convective heat transport. *J. Tiwan Inst. Chem. Engrs.* **103**, 126–137 (2019)
- M.A. Sheremet, T. Grosan, I. Pop, Free convection in a square cavity filled with a porous medium saturated by nanofluid using Tiwari and Das' nanofluid model. *Transp. Porous Media* **106**, 595–610 (2015)
- L.F. Shampine et al., Solving boundary value problems for ordinary differential equations in Matlab with Bvp4c. *Tutorial Notes* **2000**, 1–27 (2000)
- J. Kierzenka, Studies in the Numerical Solution of Ordinary Differential Equations, PhD Thesis Southern Methodist University, Dallas, TX (1998)
- J. Ahmed, M. Khan, L. Ahmad, Stagnation point flow of Maxwell nanofluid over a permeable rotating disk with heat source/sink. *J. Mol. Liq.* **287**, 110853 (2019)
- K. Naganthran, I. Hashim, R. Nazar, Triple solutions of Carreau thin film flow with thermocapillarity and injection on an unsteady stretching sheet. *Energies* **13**(12), 3177 (2020)

39. S. Bibi, Z. Elahi, A. Shahzad, Impacts of different shapes of nanoparticles on SiO_2 nanofluid flow and heat transfer in a liquid film over a stretching sheet. *Phys. Scr.* **95**(11), 115217 (2020)
40. H.I. Andersson, J.B. Aarseth, B.S. Dandapat, Heat transfer in a liquid film on an unsteady stretching surface. *Int. J. Heat Mass Transf.* **43**, 69–74 (2000)
41. C. Chen, Heat transfer in a power-law fluid film over a unsteady stretching sheet. *Heat Mass Transf.* **39**, 791–796 (2003)
42. C. Chen, Effect of viscous dissipation on heat transfer in a non-Newtonian liquid film over an unsteady stretching sheet. *J. Non-Newtonian Fluid Mech.* **135**, 128–135 (2006)
43. C. Chen, Marangoni effects on forced convection of power-law liquids in a thin film over a stretching surface. *Phys. Lett. A* **370**, 51–57 (2007)
44. C. Wang, I. Pop, Analysis of the flow of a power-law fluid film on an unsteady stretching surface by means of homotopy analysis method. *J. Non-Newtonian Fluid Mech.* **138**, 161–172 (2006)
45. Y. Lin, L. Zheng, G. Chen, Unsteady flow and heat transfer of pseudo-plastic nanoliquid in a finite thin film on a stretching surface with variable thermal conductivity and viscous dissipation. *Powder Technol.* **274**, 324–332 (2015)

Publisher's Note Springer Nature remains neutral with regard to jurisdictional claims in published maps and institutional affiliations.